

Efficient Sketch-Guided Image Inpainting via Composite Condition and Matched RoPE

Anonymous AI Frontline submission

Paper ID

Abstract

We build a complete sketch-guided image inpainting pipeline as a course project. Starting from a strong diffusion transformer baseline (FLUX.1), we systematically compare multiple ways to inject sketch control and finally adopt a parameter-efficient strategy inspired by OminiControl: we (i) construct a single composite conditional image by fusing sketch, mask, and visible pixels, avoiding an explicit mask branch; (ii) append conditional tokens to the visual token sequence; and (iii) align conditional and noisy tokens via specialized rotary positional embeddings (RoPE) so that corresponding spatial locations share identical positional phases. We fine-tune the backbone with LoRA and show that our method maintains high fidelity in the unmasked region while improving structural adherence in the inpainted region, with reduced token length and modest training cost. We also develop a paired sketch–mask–image dataset with targeted augmentations, including free-form deformation (FFD) to mimic user-drawn sketch distortions.

1. Introduction

Sketch-guided inpainting employs a model to fill a missing region of an image such that the generated content is (i) semantically consistent with a text prompt, (ii) structurally consistent with a user-provided sketch, and (iii) seamlessly blended with the visible context. Compared with text-only inpainting, sketch control introduces two practical challenges: (1) *abstraction and distortion*: user sketches are often sparse, non-photorealistic, and spatially misaligned; and (2) *efficient conditioning*: strong structure control typically requires extra networks (e.g., ControlNet-like branches) or additional input tokens, which increases compute and latency.

In this project, we aim to build a robust yet efficient system for sketch-guided inpainting. Our design starts from FLUX.1, a rectified-flow diffusion transformer operating in VAE latent space with a mixture of double-stream and

single-stream blocks and factorized 3D RoPE [1]. Inspired by OminiControl-style parameter-efficient control, we focus on how to inject sketch conditions into FLUX with minimal additional cost.

Key idea. Instead of feeding sketch and mask as separate modalities (or adding an explicit mask input branch), we build a *single composite condition image* that merges (visible) context pixels, the sketch drawn within the masked region, and the mask itself (encoded implicitly by where we place the sketch vs. original pixels). This composite condition is tokenized and appended to the visual token sequence. Crucially, we align the RoPE indices so that each conditional token and its corresponding noisy token share the same position ID, enabling direct spatial correspondence in attention. This matched RoPE alignment is the core mechanism for strong structure control without learning an additional coordinate mapping.

Contributions.

- A complete sketch-guided inpainting pipeline built on FLUX.1 with parameter-efficient training (LoRA).
- An embedded condition injection strategy: composite condition image + token concatenation + matched RoPE alignment.
- A paired sketch–mask–image dataset construction pipeline with targeted augmentations (including FFD) for robustness to sketch abstraction and misalignment.
- Empirical evaluation showing improved sketch adherence while preserving unmasked-region fidelity with reduced token length.

2. Related Work

Inpainting and diffusion-based editing. Diffusion models have become a dominant paradigm for image generation and editing. Classic inpainting pipelines often inject a binary mask explicitly, either as an extra channel or via specialized U-Net conditioning. Representative diffusion-based inpainting/editing works include RePaint [5] and

036
037
038
039

040
041
042
043
044
045
046
047
048
049
050
051
052

053
054
055
056
057
058
059
060
061
062
063
064

065
066
067
068
069
070
071

072 large-mask inpainting systems such as LaMa [9] (for non-
 073 diffusion baselines), as well as image-to-image editing ap-
 074 proaches like SDEdit [6]. These methods highlight the
 075 trade-off between control strength and computational over-
 076 head.

077 **Sketch-guided generation.** Sketch/line-conditioned edit-
 078 ing and inpainting have been explored by injecting sparse
 079 structural cues (e.g., coarse sketch lines, contours, or
 080 wireframe-like representations) into conditional generative
 081 models. DeFLOCNet [4] studies flexible low-level controls
 082 for deep image editing, and explicitly demonstrates an in-
 083 painting setting where coarse sketch lines guide the comple-
 084 tion of missing regions. For structure-critical scenes, Cao *et*
 085 *al.* [2] learn a sketch-tensor space that captures lines, edges,
 086 and junctions to improve inpainting of man-made environ-
 087 ments. In practice, such sketch-like guidance may range
 088 from clean edges to abstract strokes, so robustness to draw-
 089 ing style and spatial imprecision remains crucial.

090 **Condition injection frameworks.** ControlNet [10] and
 091 T2I-Adapter [7] popularize adding an auxiliary control
 092 branch to a frozen backbone to steer generation with edges,
 093 sketches, depth, pose, etc. While effective, extra branches
 094 increase memory and compute. OminiControl (project) em-
 095 phasizes parameter-efficient control with minimal modifica-
 096 tions, motivating our design to reuse the backbone and limit
 097 trainable parameters (via LoRA) while preserving strong
 098 spatial control.

099 **Diffusion Transformers and rectified flow.** DiT [8] re-
 100 formulates diffusion with transformers on latent tokens.
 101 FLUX.1 is a rectified-flow transformer trained in the la-
 102 tent space of an autoencoder, with mixed double-stream and
 103 single-stream blocks and factorized 3D RoPE [1]. These
 104 architectural choices influence where and how we should
 105 inject conditional tokens.

106 **Parameter-efficient fine-tuning.** LoRA [3] is widely
 107 adopted to adapt large models by learning low-rank updates
 108 to attention/MLP layers, reducing training cost. We use
 109 LoRA to fine-tune FLUX.1 for sketch-guided inpainting.

110 3. Preliminaries

111 3.1. FLUX.1 diffusion transformer

112 FLUX.1 is a rectified-flow transformer trained in the la-
 113 tent space of an image autoencoder [1]. It mixes *double-*
 114 *stream* blocks (separate weights for image and text streams,
 115 with attention applied over concatenated tokens) and *single-*
 116 *stream* blocks (a unified sequence of image and text tokens)
 117 [1]. Positional information is encoded with factorized 3D

RoPE, where each latent token is indexed by its space-time
 coordinates (t, h, w) (with $t \equiv 0$ for single images) [1]. This RoPE design is a natural handle for spatially aligned
 conditioning.

122 3.2. Sketch-guided inpainting formulation

Given an input image $\mathbf{x} \in \mathbb{R}^{H \times W \times 3}$, a binary mask $\mathbf{m} \in \{0, 1\}^{H \times W}$ (with $\mathbf{m} = 1$ indicating the *missing* region), a sketch image $\mathbf{s} \in \mathbb{R}^{H \times W \times 3}$ (or single-channel), and a text prompt c , the goal is to synthesize a completed image $\hat{\mathbf{x}}$ such that:

- $\hat{\mathbf{x}}$ matches \mathbf{x} on the visible region $(1 - \mathbf{m})$,
- $\hat{\mathbf{x}}$ respects the structure in \mathbf{s} inside \mathbf{m} , and
- the overall output is semantically consistent with c .

131 3.3. Condition injection perspective

In transformer-based diffusion, image latents are tokenized into a visual sequence. A condition can be injected by: (i) concatenating condition tokens to the visual sequence; (ii) adding cross-attention from visual tokens to condition tokens; or (iii) introducing a separate control branch. We focus on (i) because it is simple and efficient, and it matches FLUX-style “sequence concatenation” conditioning used in FLUX.1 Kontext [1].

140 4. Method

141 4.1. Overview

Our method consists of (1) composite condition image construction, (2) embedded condition injection by token concatenation, and (3) matched RoPE alignment. Figure 1 illustrates the pipeline.

146 4.2. Composite condition image

Motivation. A naive approach feeds the mask explicitly (extra channel or extra tokens) and feeds the sketch as another modality. However, explicit mask inputs increase token length and complicate architecture changes. We instead encode the mask implicitly through a *composite condition image* that uses different content in masked vs. unmasked regions.

Construction. In our formulation, the model is conditioned only on the composite image \mathbf{I}_{comp} ; therefore, an explicit binary mask is *optional*. We first present the standard full-resolution construction with an explicit mask, and then describe a more flexible “implicit-mask” variant enabled by our conditioning interface.

(A) Explicit-mask composition. Let $\mathbf{m} \in \{0, 1\}^{H \times W}$ be the binary mask, where $\mathbf{m} = 1$ indicates missing pixels. We define

$$\mathbf{I}_{\text{comp}} = (1 - \mathbf{m}) \odot \mathbf{x} + \mathbf{m} \odot \phi(\mathbf{s}), \quad (1)$$

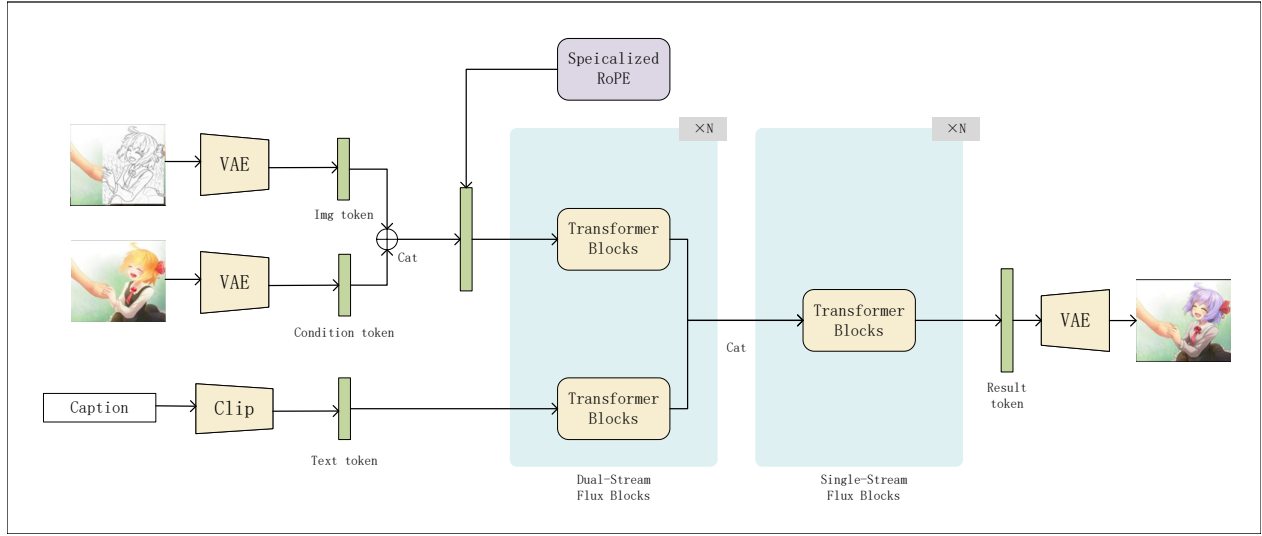


Figure 1. Method overview. We form a composite condition image by fusing the visible pixels and the sketch within the masked region, tokenize it into conditional tokens, append them to the noisy visual tokens, and apply matched RoPE alignment so that conditional and noisy tokens at the same spatial location share identical position IDs.

164 where \odot is element-wise multiplication and $\phi(\cdot)$ converts
 165 the sketch into a raster image aligned to the image canvas
 166 (e.g., replicating to 3 channels and normalizing intensities).
 167 Intuitively, the model sees ground-truth context in the un-
 168 masked region and sees sketch strokes in the masked region.

169 **(B) Implicit-mask composition via sketch placement.**
 170 Since the backbone only consumes I_{comp} , we can construct
 171 it without providing m explicitly. Let $s_0 \in \mathbb{R}^{h \times w \times 1}$ be
 172 a (possibly smaller) sketch patch and let $\mathcal{P}(\cdot; p)$ denote a
 173 placement operator that pastes the sketch patch onto a blank
 174 $H \times W$ canvas at location p (e.g., top-left corner at (u, v)),
 175 producing an aligned sketch canvas $\tilde{s} = \mathcal{P}(s_0; p)$. We then
 176 define an *implicit mask* by the support of the placed sketch:

$$\tilde{m}(i, j) = \alpha(i, j), \quad (2)$$

177 where $\alpha(i, j) \in \{0, 1\}$ denotes the alpha channel of the
 178 placed sketch canvas ($\alpha = 1$ for pixels covered by the
 179 pasted sketch strokes, and $\alpha = 0$ for transparent back-
 180 ground), and then compose

$$I_{\text{comp}} = (1 - \tilde{m}) \odot x + \tilde{m} \odot \phi(\tilde{s}). \quad (3)$$

181 In this view, “where the sketch is placed” implicitly specifies
 182 the region to be edited, making the explicit mask input
 183 unnecessary when users provide localized sketches.

186 **Why this helps.** This design encourages the model to (i)
 187 preserve the unmasked region by directly providing it as
 188 condition, and (ii) interpret strokes as a structural hint for
 189 missing content. Compared with explicit-mask designs, we
 190 reduce the need for a separate mask-processing pathway

191 and can reduce effective input length in some injection vari-
 192 ants (see Sec. 4.6): when an explicit-mask baseline injects
 193 both a sketch condition sequence and a separate mask se-
 194 quence (each tokenized to N latent tokens), the additional
 195 tokens scale as $N_{\text{extra}} = N_{\text{sketch}} + N_{\text{mask}} = 2N$, whereas
 196 our composite condition uses a *single* condition sequence
 197 ($N_{\text{extra}} = N$), yielding a 50% reduction in extra condition
 198 tokens.

4.3. Embedded condition injection via token concatenation

201 Following FLUX-style conditioning, we encode I_{comp} into
 202 VAE latents and tokenize it into a conditional token se-
 203 quence T_{cond} . Let T_{noisy} denote the noisy latent tokens at
 204 diffusion time t . We form a visual sequence by concatena-
 205 tion:

$$S_{\text{visual}} = \text{Concat}(T_{\text{noisy}}, T_{\text{cond}}), \quad (4)$$

207 and then proceed with the FLUX blocks. In FLUX.1,
 208 double-stream blocks treat text and image streams sepa-
 209 rately and interact via attention mechanisms, while single-
 210 stream blocks process a unified sequence [1]. We adapt the
 211 injection to both stages:

- **Double-stream stage:** T_{cond} participates in the image stream attention early, helping establish the global structure topology.
- **Single-stream stage:** T_{cond} , T_{noisy} , and text tokens attend jointly, enabling deep fusion of structure (sketch) and semantics (prompt).

218 4.4. Matched RoPE alignment

219 **Key mechanism.** We align positional indices between
 220 conditional and noisy tokens. Concretely, instead of assigning
 221 new position IDs to conditional tokens, we force them to
 222 reuse the position IDs of their spatially corresponding
 223 noisy tokens. This makes the RoPE phase identical for a
 224 pair of tokens at the same spatial location, enabling attention
 225 to directly couple “current pixel” and “corresponding
 226 sketch” without learning an additional spatial transform.

227 **Implementation sketch.** Let a token at spatial location
 228 (h, w) have a RoPE index $\pi(h, w)$. For each (h, w) , we
 229 set:

$$\pi_{\text{cond}}(h, w) := \pi_{\text{noisy}}(h, w). \quad (5)$$

231 4.5. Training objective and LoRA fine-tuning

232 We keep the original rectified-flow / flow-matching objec-
 233 tive of the FLUX backbone and fine-tune with LoRA. Let
 234 \mathbf{z}_t be a noised latent at time t and $\mathbf{v}_\theta(\cdot)$ be the predicted
 235 velocity/flow field. We optimize a flow matching loss:

$$\mathcal{L}_{\text{FM}} = \mathbb{E}_{t, \epsilon} \left[\|\mathbf{v}_\theta(\mathbf{z}_t, t; c, \mathbf{I}_{\text{comp}}) - \mathbf{v}^*\|_2^2 \right], \quad (6)$$

237 where \mathbf{v}^* is the target velocity under the chosen rectified-
 238 flow parameterization.

239 We apply LoRA adapters to attention projections. This
 240 allows fast fine-tuning while keeping most backbone
 241 weights frozen.

242 4.6. Efficiency discussion

243 Our design is efficient in three senses:

- 244 • **No extra control branch:** unlike ControlNet-style add-
 245 on networks, we reuse the backbone and only introduce
 246 LoRA parameters.
- 247 • **Simple conditioning interface:** we use token concatenation,
 248 consistent with FLUX-style sequence construction
 249 [1].
- 250 • **Reduced explicit inputs:** the mask is not injected as a
 251 separate explicit modality; instead it is encoded implicitly
 252 via the composite condition image, which can reduce
 253 extra tokens/channels needed by some baselines.

254 5. Dataset Preparation

255 5.1. Paired sketch–mask–image construction

256 We construct training triplets $(\mathbf{x}, \mathbf{m}, \mathbf{s})$ with the following
 257 goals: (1) diverse object categories and complex scenes, (2)
 258 sketches that resemble human drawings rather than perfect
 259 edges, and (3) masks that simulate realistic user edits.

260 **Hybrid training sources.** We firstly try to adapt existing
 261 datasets to our tasks, like FSCOCO and SketchyScene, but

then we find these datasets are originally intended for drawing from scratch, which has already been achieved by previous works. So we trained them on these datasets to preemptively evaluate the capability of OminiControl Training Framework, which has satisfying results Figure 1.

262 But when it comes to fitting the 2 datasets for our specific
 263 task, problems arises as the sketches are either too roughly
 264 drawn by hand or semantically irrelevant as generated by
 265 AI so that we failed to extract the main objects from them,
 266 for which reason wo cannot build the sketch-implanted im-
 267 ages we needed for our specific tasks. Therefore, we shift
 268 our minds and discover anime images are always a cou-
 269 ple of characters that are distinctively standing out against
 270 the background, so we choose the Dabooru Datasets as our
 271 training dataset source.

272 As the dataset is crawled from Dabooru, a original amine
 273 image board, the images are of varying quality. So we ap-
 274 pply Image Quality Assessment (IQA) metrics to filter the
 275 images on technical distortions (like blur, noise, and com-
 276 pression artifacts), structural integrity, and aesthetic appeal.

277 **Object-centric masking and sketch acquisition.** To en-
 278 able semantic-level alignment training with the filtered
 279 Danbooru dataset, we leverage a segmentation model
 280 (SAM3) in preprocessing. Given an image, the SAM3 pro-
 281 poses object-level regions (in our case, heads/characters)
 282 and helps associate sketches with bounding boxes of the
 283 highest confidence. We then apply segmentation to ex-
 284 tract object masks and define the inpainting region \mathbf{m} in an
 285 object-centric manner. As a results, the head/character re-
 286 gion on the original image is replaced with the sketch region
 287 $\tilde{\mathbf{m}}$.

288 5.2. Sketch robustness augmentations

289 Real user sketches are often misaligned and distorted. To
 290 improve robustness, we apply a single targeted augmen-
 291 tation during training: **non-rigid free-form deformation**
 292 (**FFD**). Specifically, we warp sketch strokes using a coarse
 293 control lattice with smooth interpolation, which mimics
 294 hand-drawn proportion errors and local shape drift while
 295 preserving the overall topology. This augmentation discour-
 296 ages the model from memorizing pixel-precise sketch co-
 297 ordinates and encourages more semantic use of structural
 298 cues.

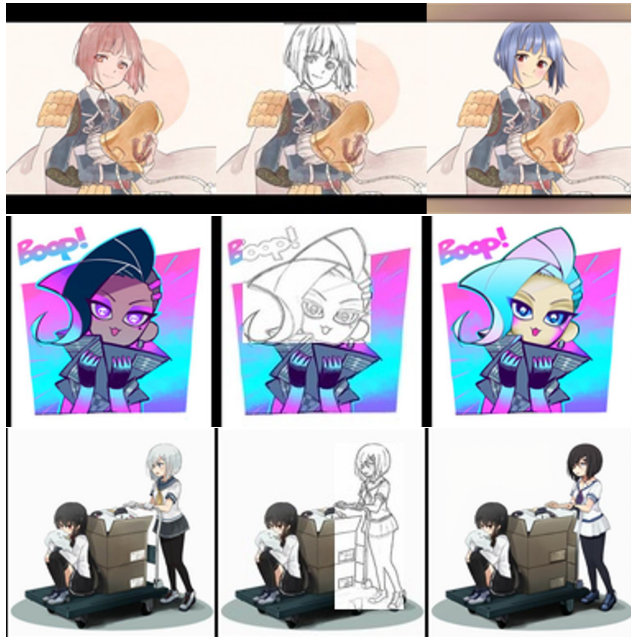
299 6. Experimental Setup

300 6.1. Baselines

301 We mainly compare 2 ways to inject sketch guidance into
 302 FLUX-like backbones:

- 303 • **Text-only inpainting:** We evaluate FLUX under a mask-
 304 conditional setting without sketch constraints. Our em-
 305 pirical findings indicate two primary failure modes: (1)

Partial inpainting on danbooru



Full-mask inpainting on fscoco

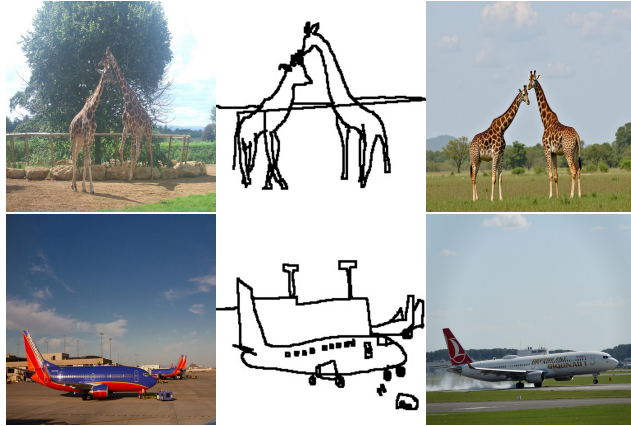


Figure 2. Qualitative results on danbooru (top) and fscoco (bottom). Each example is organized as *input image | sketch/condition | ours*. Our method faithfully restores the missing regions for small masks while preserving global semantics and structure for full-mask generation, producing coherent textures and natural transitions along mask boundaries.

prompt-alignment degradation, where the model fails to strictly follow complex or long-context text instructions; and (2) descriptive ambiguity, where the intended filling region involves irregular shapes or textures that exceed the expressive capacity of natural language prompts.

• Ours: To address the baseline limitations, we employ a composite conditioning strategy that integrates structural guidance (sketches) via image implantation. Crucially, we implement Matched RoPE Alignment: instead of ap-

Table 1. Quantitative results on danbooru dataset.

Method	PSNR \uparrow	SSIM \uparrow	FID \downarrow
Ours	15.40	0.78	76.20

pending sequential positions, we assign the condition tokens the exact same rotary positional indices as the target latents. This enforces strict spatial correspondence between the structural condition and the generated output.

6.2. Training details

We fine-tune FLUX.1 with LoRA. Unless otherwise specified, we use: optimizer Prodigy, learning rate 1.0 (with Prodigy) weight decay 0.01, LoRA rank 16, resolution 512*512, and 5,000 training steps for head-sketch implantation and 10,000 training steps for character-sketch implantation, with a flow matching (rectified flow) loss.

6.3. Evaluation metrics

We report PSNR and SSIM to measure pixel-level fidelity and structural similarity, and we also report FID to reflect perceptual realism and distributional similarity between generated outputs and real images. All metrics are computed on the final inpainted images over the evaluation set.

7. Results

7.1. Qualitative results

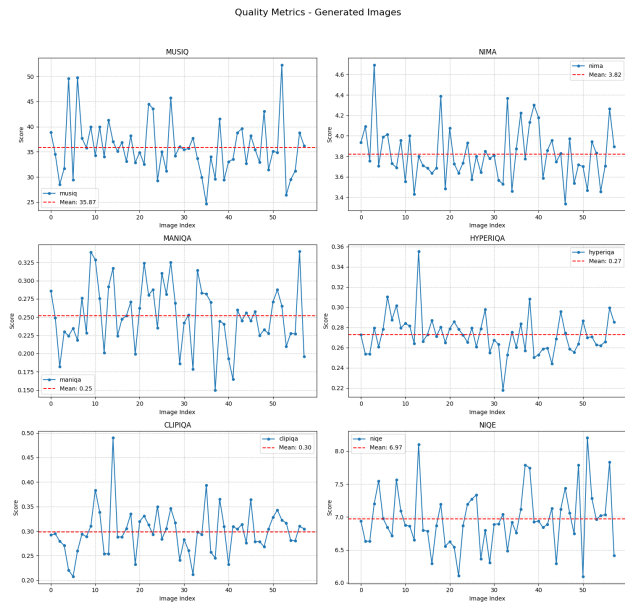
Figure 2 presents representative results on Danbooru (partial masks) and FSCOCO (full masks). Across examples, our method better follows sparse and abstract strokes inside the masked region while keeping the visible context nearly unchanged. We also observe cleaner transitions along mask boundaries, suggesting that the composite condition helps preserve global consistency and prevents unintended edits outside the target region. Notably, even when sketches contain crossings or mild spatial distortion, matched RoPE alignment encourages location-wise correspondence between conditional and noisy tokens, yielding more plausible structure completion. Figure 3

7.2. Quantitative results

We report PSNR/SSIM to quantify fidelity on the visible (unmasked) region, and FID to reflect perceptual realism of the final outputs. Table 1 summarizes the results on danbooru dataset. Since our project focuses on an efficient condition-injection design and is trained at a course-project scale, we include these metrics as a reference for overall quality; a more exhaustive quantitative comparison against strong sketch-control baselines is left for future work.



(a) Metrics for Original Images



(b) Metrics for Generated Images

Figure 3. Comparative analysis of IQA scores between original and generated datasets.

361

7.3. Ablation studies

362 We conduct ablations to isolate the effect of each component:
363

- 364 • **Without composite condition:** feed sketch alone
365 (masked region not distinguished), leading to weaker
366 preservation of context and occasional artifacts.
- 367 • **Without matched RoPE:** assign independent position



Figure 4. **Failure case due to misalignment.** The figure demonstrates the model’s behavior when the sketch implantation is not perfectly aligned with the underlying image. The spatial discrepancy between the provided sketch (middle) and the original structure leads to distortion in the final generation (right).

IDs to condition tokens; we observe degraded structural control, especially under sketch misalignment.

- **Without FFD augmentation:** the model overfits to “clean” sketch geometry and becomes brittle to user-like distortions.

8. Discussion

8.1. Why matched RoPE alignment works

Matched RoPE alignment makes spatial correspondence explicit at the positional-encoding level. In attention, tokens at the same spatial location share the same RoPE phase, encouraging the model to learn a direct mapping between the current latent state and the intended structure implied by the sketch. This is particularly useful when sketches are sparse: the model can propagate structural constraints via global attention while still grounding them spatially.

8.2. Failure cases and limitations

Our model can still fail when sketches are extremely symbolic (e.g., stick figures) or when the sketch implantation is not perfectly aligned with the image Figure 4. We also observe that overly long or repeated edits (multi-turn) can accumulate artifacts (a general limitation in interactive editing models).

8.3. Practical notes for a course project

We prioritize a clean, reproducible pipeline and parameter-efficient training over exhaustive scaling. This choice keeps engineering complexity manageable while still enabling meaningful exploration of condition injection designs.

9. Conclusion

We presented a sketch-guided inpainting system built on FLUX.1 with an efficient control mechanism inspired by OminiControl. Our key design—composite condition image, token concatenation, and matched RoPE alignment—provides strong structural control while preserving unmasked-region fidelity, with modest training

368
369
370
371
372

373

374

375
376
377
378
379
380
381
382

383

384
385
386
387
388
389

390

391
392
393
394

395
396
397
398
399
400
401

402 overhead using LoRA. We also described a dataset con-
403 struction and augmentation pipeline (including FFD) to im-
404 prove robustness to sketch abstraction and distortion. Fu-
405 ture work includes controllable “roughness” (faithfulness-
406 to-sketch) and extending to multi-condition control (e.g.,
407 depth/pose) in a unified interface.

408 References

- 409 [1] Black Forest Labs. Flux.1 kontext: Flow matching for in-
410 context image generation and editing in latent space. *arXiv*
411 preprint arXiv:2506.15742, 2025. 1, 2, 3, 4
- 412 [2] Chen Cao and (CVF). Learning a sketch tensor space for
413 image inpainting of man-made scenes. In *Proceedings of*
414 *the IEEE/CVF International Conference on Computer Vision*
415 (*ICCV*), 2021. 2
- 416 [3] Edward J. Hu, Yelong Shen, Phillip Wallis, Zeyuan Allen-
417 Zhu, Yuanzhi Li, Shean Wang, and Weizhu Chen. Lora:
418 Low-rank adaptation of large language models. *arXiv*
419 preprint arXiv:2106.09685, 2021. 2
- 420 [4] Hongyu Liu, Ziyu Wan, Wei Huang, Yibing Song, Xintong
421 Han, Jing Liao, Bing Jiang, and Wei Liu. Deflocnet: Deep
422 image editing via flexible low-level controls. In *Proceedings*
423 *of the IEEE/CVF Conference on Computer Vision and Pat-*
424 *tern Recognition (CVPR)*, 2021. 2
- 425 [5] Andreas Lugmayr, Martin Danelljan, Andres Romero, Fisher
426 Yu, Radu Timofte, and Luc Van Gool. Repaint: Inpainting
427 using denoising diffusion probabilistic models. In *Proceed-*
428 *ings of the IEEE/CVF Conference on Computer Vision and*
429 *Pattern Recognition (CVPR)*, 2022. 1
- 430 [6] Chenlin Meng, Yutong He, Yang Song, Stefano Ermon, Jia-
431 jun Wu, and Serge Belongie. Sdedit: Guided image synthe-
432 sis and editing with stochastic differential equations. *arXiv*
433 preprint arXiv:2108.01073, 2021. 2
- 434 [7] Chong Mou, Xiantao Zhang, Zhaoyang Li, and others. T2i-
435 adapter: Learning adapters to dig out more controllable abil-
436 ity for text-to-image diffusion models. In *Proceedings of*
437 *the AAAI Conference on Artificial Intelligence*, pages 4296–
438 4304, 2024. 2
- 439 [8] William Peebles and Saining Xie. Scalable diffusion mod-
440 els with transformers. In *Proceedings of the IEEE/CVF In-*
441 *ternational Conference on Computer Vision (ICCV)*, pages
442 4172–4182, 2023. 2
- 443 [9] Roman Suvorov and others. Resolution-robust large mask
444 inpainting with fourier convolutions. In *Proceedings of the*
445 *IEEE/CVF Winter Conference on Applications of Computer*
446 *Vision (WACV)*, 2022. 2
- 447 [10] Lvmin Zhang and Maneesh Agrawala. Adding conditional
448 control to text-to-image diffusion models. In *Proceedings of*
449 *the IEEE/CVF International Conference on Computer Vision*
450 (*ICCV*), 2023. 2